J. Mt. Sci. (2014) 11(6): 1571-1578 e-mail: jms@imde.ac.cn http://jms.imde.ac.cn
DOI: 10.1007/s11629-013-2769-3

Effects of Heat Softening on Initiation of Landslides

XIONG Chuan-xiang[1,2*], LU Xiao-bing[3], HUANG Wei-da[4], WANG Cheng-hua[5]

1 School of Environment and Resources, Fuzhou University, Fuzhou 350108, China

2 Fujian Provincial Key Laboratory of Remote Sensing of Soil Erosion and Disaster Protection, Fuzhou 350108, China

3 Institute of Mechanics, Chinese Academy of Sciences, Beijing 100190, China

4 Fujian Academy of Building Research, Fuzhou 350025, China

5 Institute of Mountain Hazards and Environment, Chinese Academy of Sciences, Chengdu 610041, China

**Corresponding author, e-mail: xiongchx@aliyun.com*

Citation: Xiong CX, Lu XB, Huang WD, et al. (2014) Effects of heat softening on initiation of landslides. Journal of Mountain Science 11(5). DOI: 10.1007/s11629-013-2769-3

Abstract: Effects of heat softening on the initiation of slide surface (shear banding) in clayey slopes during fast deformation were discussed. Controlling equations considering heat, pore pressure and mechanical movement were presented. By perturbation method, the instability condition of localized zone (i.e. criterion for initiation of shear banding) for thermal related soils, such as clayey slope, was obtained. It is shown that slide surface initiates once the thermal-softening effects overcome the strain-hardening effects whether it is adiabatic or not. Without strain hardening effects, strain rate hardening obviously plays a role in initiation of shear band. During initiating process, heat is trapped inside the shear band, which leads rapidly to a pore pressure increase and fast loss of strength. The localized shear strain is concentrated in a narrow zone with a width of several centimeters at most and increases fast. This zone forms the sliding surface. Temperature can increase more than 2°C, pore pressure can increase 160% in about 0.1s inside this zone. These changes cause the fast decrease in friction-coefficient by about 36% over the initial value. That is how shear band initiated and developed in clayey slopes.

Keywords: Landslide; Thermo-effect; Slide surface; Initiation

Received: 2 May 2013
Accepted: 17 January 2014

Introduction

It is observed that many landslides undergo a large slip in a localized zone before catastrophic failure. Shear localization in a rock or soil layer occurs in very narrow zones of few centimetres thick or even less. As the localized zones are very thin, besides the pore water seepage, thermal effects during rapid slip may be of primary importance (Jean et al. 2011). For example, disastrous Vaiont slide happening on 9 October 1963 showed to be a collapse after a long-term creep during which a localized zone was formed in clay-rich layers with 0.005 to 0.175 m thick, embedded in the limestone (Figure 1) (Veveakis et al. 2007). The clay-rich layer was heated during creep. The maximum temperature rise can be 2.5°C for clayey siltstones if shear rate is greater than 0.1 m/min. Meanwhile significant loss of static strength can be up to 60% (Tika and Hutchinson 1999). The dynamic friction angle of the clayey sample of Vaiont slide may decrease to φ_{dyn}=4.4°. In fact, the temperature rise can be 5°C when the predominant mineral is montmorillonite (Moor 1991). So fault zones commonly exhibit the presence of fluid interacting with the rock, and thus coupled effects including shear heating and pore pressure are expected to play a role as weakening

mechanisms during fault slip. These mechanisms have also been suggested for weakening in catastrophic landslides (Rice 2006; Lu 2010).

Some researchers think that the decrease of slope strength resulted from high speed landslide is caused by thermal-induced vaporization (Hibib 1975; Goguel 1978). Nevertheless, no evidence of vaporization is found either in site or in experiments. Voight et al. (1982) showed that even if there was no vaporization, high pore pressure may be induced by thermal in shear band by a one-dimensional slide-blocks mechanical model. At the same time, there are many discussions about the relation between the pressure of pore fluid and the friction-induced thermal and melting which are related to strong seism (Lachenbruch 1980; Mass 1985). A set of equations were presented to describe the high movement of shear band in landslide in which the width of shear band is assumed to be fixed (Vardoulikas 2000, 2002).

In this paper, the course and mechanism of thermal-induced landslide of a slope rich in clay are investigated. The generation of heat during shear and the effects of heat on the friction coefficients and pore pressure are discussed.

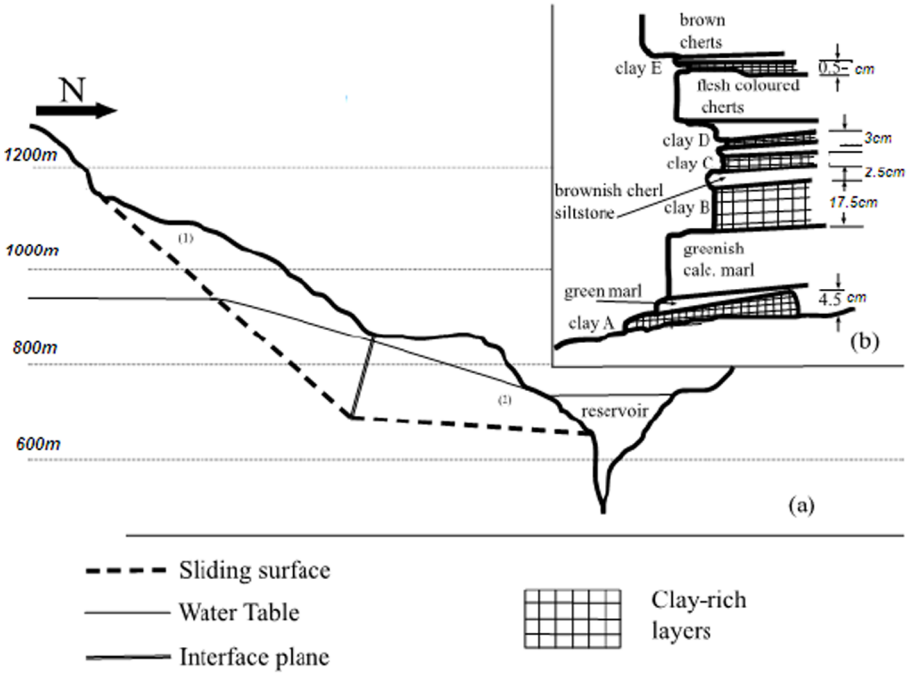

Figure 1 Geology of the Vaiont slide. (a) "Chair" failure mechanism of the Vaiont slide. The back of the chair is assumed to dip at 40.5°, while the seat is almost horizontal, dipping at 2.5°. (b) Stratigraphy of the rocks of the Vaiont sliding surface. This sequence is found in outcrops in the Vaiont area at the same stratigraphic position as those at the base of the Vaiont slide. Slip is thought to have been confined in the clay-rich layers. To the right, thickness is given in centimeters. Redrawn from Veveakis et al. (2007).

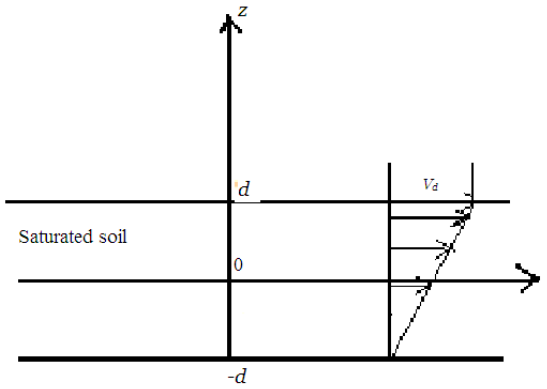

Figure 2 sketch of the problem V_d.

1 Formulation of Problem

According to the observation, the failure plane is in reality a thin band of rapidly deforming soil, whereas the sliding body (layer over the failure plane) itself is moving as a rigid body at least in the early stage (Tika and Hutchinson 1999). Because of this big difference between the shear band thickness and the characteristic length of the sliding body, we can split the problem into two subproblems: (1) Rapid developing of shear band. (2) rigid-body motion of sliding body. Here we discuss only the first one: initiation and evolution of a long deforming shear band in saturated clayey soils. The considered zone has a thickness of 2d. Inside this zone temperature, pore pressure and deformation are assumed to be function only of time and coordinate Z, normal to the band direction (Figure 2). At the boundary, the velocity is v_d which is induced by the movement of rigid

body above it. It is assumed fully permeable to pore fluid and fully conductive to heat flux at the shear band boundary. The bottom of the zone is fixed.

During fast shearing, the diffusion equation for the pore pressure is obtained from the fluid mass balance equation and is expressed as the sum of three terms: the diffusion term, the thermal pressurization term, and the term corresponding to the effect on pore pressure of inelastic porosity change (Jean et al. 2011):

$$\frac{\partial p}{\partial t}=\frac{\partial}{\partial z}\left(C_v\frac{\partial p}{\partial z}\right)+\lambda_m\frac{\partial \theta}{\partial t}-\frac{1}{\beta}\frac{\partial n}{\partial t} \tag{1}$$

in which C_v is consolidation coefficient, λ_m pore-pressure-temperature coefficient determined by thermal expansion coefficient and compression, β the storage capacity, n the porosity.

Assuming that the changes in porosity are mainly due to shear (dilatancy law), we will have:

$$\frac{\partial n}{\partial t}=-C_s\frac{\partial \gamma}{\partial t} \tag{2}$$

Assuming that the pore pressure and the grains of clay is in the thermal equilibrium state, heat equation of diffusion-generation may be obtained by energy equilibrium:

$$\rho c\frac{\partial \theta}{\partial t}=\lambda\frac{\partial^2\theta}{\partial z^2}+f\tau\dot{\gamma}^p \tag{3}$$

ρ =(1-n)ρ_s, ρ_s is the densities of soil, and c the heat capacity, λ the thermal conductivity, θ the temperature, f the work-thermal transition coefficient, τ the shear stress, $\dot{\gamma}^p$ the plastic shear strain. In the next discussion of this paper, it is assumed that elastic shear strain may be neglected since it is much smaller than the plastic strain, thus

$$\dot{\gamma}^p\approx\dot{\gamma}=\frac{\partial v}{\partial z}$$

Assuming that clayey soils is applied on simple shearing and considering the interaction between skeleton and pore water, the momentum equilibrium equation is proposed as follows(Lu et al. 2001):

$$\rho\frac{\partial^2\gamma}{\partial t^2}-\frac{\partial^2\tau}{\partial z^2}=-Kn^2\frac{\partial \gamma}{\partial t} \tag{4}$$

in which n is the porosity, K equals to μ/k, with μ being the viscosity of water and k the physical permeability. The first term on the left side is inertial and the second term shear stress. The term on the right side of Eq.(4) indicates the resistance between water and soil skeleton. For soils, such as clay, the resistance is very small because the relative velocity is very small. So this term is neglected in the following.

Generally, the mathematical formulation of the problem is as follows:

$$\begin{cases}\rho\dfrac{\partial^2\gamma}{\partial t^2}-\dfrac{\partial^2\tau}{\partial z^2}=0\\ \rho c\dfrac{\partial\theta}{\partial t}=\lambda\dfrac{\partial^2\theta}{\partial z^2}+f\tau\dot{\gamma}\\ \dfrac{\partial p}{\partial t}=C_v\dfrac{\partial^2 p}{\partial z^2}+\lambda_m\dfrac{\partial\theta}{\partial t}+a\dfrac{\partial\gamma}{\partial t}\end{cases} \tag{5}$$

in which a=Cs/β.

Shear stress is thought to be determined by shear strain, shear strain rate and temperature, the constitutive relation is as follows:

$$\tau=f(\gamma,\dot{\gamma},\theta) \tag{6}$$

2 Perturbation Analysis

In order to find the instability conditions of shearing, we investigate the following solutions:

$$\begin{cases}\gamma=\gamma_0+\gamma';|\gamma'|<<|\gamma_0|\\ \theta=\theta_0+\theta';|\theta'|<<|\theta_0|\\ p=p_0+p';|p'|<<|p_0|\end{cases}\ \text{and}\ \begin{cases}\gamma'=\gamma^*e^{\alpha t+i\beta z}\\ \theta'=\theta^*e^{\alpha t+i\beta z}\\ p'=p^*e^{\alpha t+i\beta z}\end{cases} \tag{7}$$

in which γ_0,θ_0,p_0 are a set of solution of Eq. (5), α, β are the perturbation frequency and wave number, $\gamma^\bullet,\theta^\bullet,p^\bullet$ are perturbation amplitudes of strain, temperature and pore pressure, respectively.

For dense soils considered in this paper, shear generally makes materials dilatant and the strength increases while heat is on the contrary. By differentiating of equation (6), the following equation can be obtained:

$$d\tau=R_0d\gamma-Q_0d\theta+H_0d\dot{\gamma} \tag{8}$$

in which

$$R_0=\left(\frac{\partial\tau}{\partial\gamma}\right)_0,Q_0=-\left(\frac{\partial\tau}{\partial\theta}\right)_0,H_0=\left(\frac{\partial\tau}{\partial\dot{\gamma}}\right)_0 \tag{9}$$

Thus

$$\tau^\bullet=R_0\gamma^\bullet-Q_0\theta^\bullet+\alpha H_0\gamma^\bullet \tag{10}$$

in which R_o indicates strain hardening, Q_o heat softening, H_o strain rate hardening.

Instituting Eq.(7) and Eq.(10) into Eq.(5), the following homogeneous system of equations may be obtained:

$$\begin{cases} \left[\rho\alpha^2+\beta^2(R_0+\alpha H_0)\right]\dot{\gamma}^{\bullet}-\beta^2 Q_0\theta^{\bullet}=0 \\ \left[f\tau_0\alpha+f\dot{\gamma}_0(R_0+\alpha H_0)\right]\dot{\gamma}^{\bullet}-\left(f\dot{\gamma}_0 Q_0+\rho c\alpha+\lambda\beta^2\right)\theta^{\bullet}=0 \\ a\alpha\dot{\gamma}^{\bullet}+\lambda_m\alpha\theta^{*}-\left(\alpha+C_v\beta^2\right)p^{*}=0 \end{cases} \tag{11}$$

It is clear that if the system has solutions, the determinant of the coefficients should be equal to zero, which leads to:

$$\rho\alpha^3+A_1\alpha^2+A_2\alpha+k_m R_0\beta^4=0 \tag{12}$$

in which $A_1=\rho f\dot{\gamma}_0 Q_0+\left(\rho\lambda+\rho c H_0\right)\beta^2$,

$A_2=\lambda H_0\beta^4+\left(\rho c R_0-f Q_0\tau_0\right)\beta^2$

Now, the dimensionless form of Eq. (12) can be obtained by the following dimensionless parameters:

$$\begin{cases} \alpha=\dfrac{cR_0}{\lambda}\bar{\alpha},\beta^2=\dfrac{R_0c^2\rho}{\lambda^2}\bar{\beta}^2,A=\dfrac{f\dot{\gamma}_0 Q_0\lambda}{\rho c^2 R_0}, \\ B=\dfrac{H_0 c}{\lambda},C=\dfrac{H_0}{R_0},D=\dfrac{fQ_0\tau_0}{pcR_0} \end{cases} \tag{13}$$

In this way, Eq. (12) can be rewritten as follows:

$$\bar{\alpha}^3+\left[A+\bar{\beta}^2(1+B)\right]\bar{\alpha}^2+\left[(1-D)\bar{\beta}^2+C\bar{\beta}^4\right]\bar{\alpha}+\bar{\beta}^4=0 \tag{14}$$

In the same way of literature (Lu et al. 2001), we can obtain the instability condition:

$$\frac{f\tau_0 Q_0}{\rho cR_0}>1 \tag{15}$$

The above equation shows that the instability condition occurs when the effects of thermal softening overcome the effects of strain hardening. That means, temperature rises with shearing, causing the strength decay, while strain increase makes the strength rise. In some cases, effects of heat softening rise faster than that of effects of strain hardening, the strength will be lost and instability occurs. After instability, the band width of localized shear evolves with the changes of pore pressure and temperature inside the band.

In adiabatic conditions, λ=0, Eq.(12) becomes

$$\rho^2 c\alpha^2+\left(\rho f\dot{\gamma}_0 Q_0+\rho c H_0\beta^2\right)\alpha+\left(\rho cR_0-fQ_0\tau_0\right)\beta^2=0 \tag{16}$$

If $\rho_c R_o$-$fQ_o\tau_o$<0, it is certain that α has a positive root and the instability must occur. It is interesting that the same criterion (15) can be used whether the instability is adiabatic or not. That means, instability is not related with adiabatic condition. According to Eq.(4), heat transferring can only delay the occurrence of instability.

If R_o=0, means no strain hardening, the instability condition can be obtained as follows by Eq.(12):

$$\lambda H_0\beta^2-fQ_0\tau_0<0 \tag{17}$$

It means in this case the thermal softening effect must overcome the strain rate hardening effect.

If Q_o=0, it means no thermal softening, only in case of R_o<0, instability can occur. In this case, liquefaction may occur but without localization because the soil is now strain softening material.

From the results above, heat is a key in the localization instability of clayey soils that heat can be induced by friction. Localized shear banding will start when heat -induced softening is larger than that of strain-induced hardening. As for other kinds of soils which are not related with heat, instability mechanism is determined by other factors.

3 Evolution of Band Width and its Effects on the Pore Pressure

3.1 Simplification of mathematical model

Now, p, θ, γ are solved numerically under the condition of simple constitutive relation, to understand the phenomenon of shear → thermal → pore pressure → friction softening.

The following dimensionless equations may be obtained by Eq.(5):

$$\begin{cases} \dfrac{\delta_k^2\dot{\gamma}_k}{\tau_k t_k}\dfrac{\partial\bar{\dot{\gamma}}}{\partial\bar{t}}-\dfrac{\partial^2\bar{\tau}}{\partial\bar{z}^2}=0 \\ \dfrac{\partial\bar{\theta}}{\partial\bar{t}}=\dfrac{\partial^2\bar{\theta}}{\partial\bar{z}^2}+\dfrac{f\bar{\tau}\bar{\dot{\gamma}}}{2} \\ \dfrac{\partial\bar{p}}{\partial\bar{t}}=\dfrac{C_v t_k}{\delta_k^2}\dfrac{\partial^2\bar{p}}{\partial\bar{z}^2}+\dfrac{\lambda_m\theta_k}{p_k}\dfrac{\partial\bar{\theta}}{\partial\bar{t}}+\dfrac{a\dot{\gamma}_0 t_k}{p_k}\bar{\dot{\gamma}} \end{cases} \tag{18}$$

with the dimensionless parameters: $\bar{p}=p/p_k$, $\bar{\theta}=\theta/\theta_0$, $\bar{\dot{\gamma}}=\dot{\gamma}/\dot{\gamma}_k$, $\bar{\tau}=\tau/\tau_k$, $\bar{t}=t/t_k$, $\bar{y}=y/\delta_k$, the parameters with subscript denote the corresponding characteristic parameters. For example, P_k is the characteristic pore pressure, and δ_k the half thickness of shear band. t_k and $\delta^2{}_k$ are adopted as $\lambda\delta_k^2/(2\rho c)$ and $\tau_k\dot{\gamma}_0/(\lambda\theta_0)$, respectively.

With $\rho_s \sim 10^3 kg/m^3$, $k_m \sim 10^{-7} m^2/s$, $\theta_k \sim 10^{1\sim2^\circ} C$, $\tau_k \sim 10^{6\sim7} Pa, \dot{\gamma}_k \sim 10^{-1}/s$, $p_k \sim 10^{5\sim6} Pa$, $C_v \sim 10^{-7} m^2/s$, $\lambda_m \sim 10^4 Pa/^\circ C$, the small-quantity $\delta_k^2 \dot{\gamma}_k / (\tau_k t_k)$ leads to Eq. (18) simplified as Eq.(19). In the following sections, the symbol "—"is omitted for convenient expression.

In this way, the controlling equations of saturated sand under confined conditions are as follows:

$$\begin{cases} \dfrac{\partial^2 \bar{\tau}}{\partial \bar{z}^2} = 0 \\ \dfrac{\partial \bar{\theta}}{\partial \bar{t}} = \dfrac{\partial^2 \bar{\theta}}{\partial \bar{z}^2} + \dfrac{f \bar{\tau} \bar{\dot{\gamma}}}{2} \\ \dfrac{\partial \bar{p}}{\partial \bar{t}} = \dfrac{C_v \lambda}{\rho c} \dfrac{\partial^2 \bar{p}}{\partial \bar{z}^2} + \dfrac{\lambda_m \theta_k}{p_k} \dfrac{\partial \bar{\theta}}{\partial \bar{t}} + \dfrac{a \dot{\gamma}_0 t_k}{p_k} \bar{\dot{\gamma}} \end{cases} \tag{19}$$

$$z = 0, \frac{\partial \theta}{\partial z} = 0 \tag{19a}$$

$$z = \delta(t), \theta_{\delta_-} = \theta_{\delta_+} \tag{19b}$$

$$\frac{\partial \theta}{\partial z}|_{\delta_-} = \frac{\partial \theta}{\partial z}|_{\delta+} \tag{19c}$$

$$v|_{\delta_-} = RV(t) \tag{19d}$$

$$t = 0, \theta = \theta_0(z) \tag{19e}$$

in which $R = v_0 / \delta_k \dot{\varepsilon}_k$, $\theta_0(z)$ and v_o are the initial temperature and the initial velocity respectively, *V(t)* is the dimensionless boundary velocity and *V*=1 when *t*=0.

According to the analysis in literature (Lu et al. 2005), the diffusion of pore pressure causes the shear band expanding, while the development of strain causes the shrinking of shear band on a linear assumption of constitutive relation.

3.2 Numerical simulation

Generally, the constitutive relation of soils is nonlinear. To study the evolution of shear band and its effects on landslide in this case, numerical simulation is carried out based on Eq. (19). The constitutive relation is adopted as the following form:

$$\tau = A \gamma^m \dot{\gamma}^n \theta^l \tag{20}$$

Such a problem is investigated here: A thin clayey soil layer is beneath a thick rigid rock or soil. The rigid layer drives the thin clayey soil to move. Heat will form and localization may form. Development of temperature and pore pressure and displacement will be simulated to investigate the effects of main factors on initiation and evolution of shear band. A sliding surface located at about 200m below the slope surface which is formed by a thin layer of clayey layer. Shear band occurred and developed in this layer. The parameters and numerical results are all regularized in dimensionless form. In such way, the results can be used in other cases whose dimensionless parameters are in the same range. In simulation, the parameters of the slope are determined mainly by reference of Vaiont slide (Veveakis et al. 2007; Tika and Hutchinson 1999) which are as follows: E_r=1×10^{5}Pa, ρ=2.4×10^{3}kg/m^3, a=1.0, f=1.0, A=1000.0, m=0.1, n=0.1, l=-5.0, P_k=3×10^{5}Pa, τ_k=1×10^{6}Pa, p_o=1×10^{6}Pa, $\dot{\gamma}_0$ =1×10^{-5}/s, θ_o=22°C

The initial strain-rate at the center point is 5% higher than that at other points.

From Figures 3 and 4, it can be seen that strain, strain-rate and heat are concentrated in a narrow zone with a width of several centimeters at

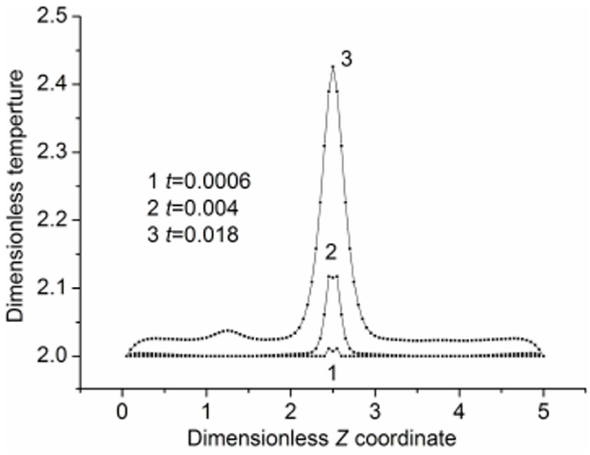

Figure 3 Changes of temperature.

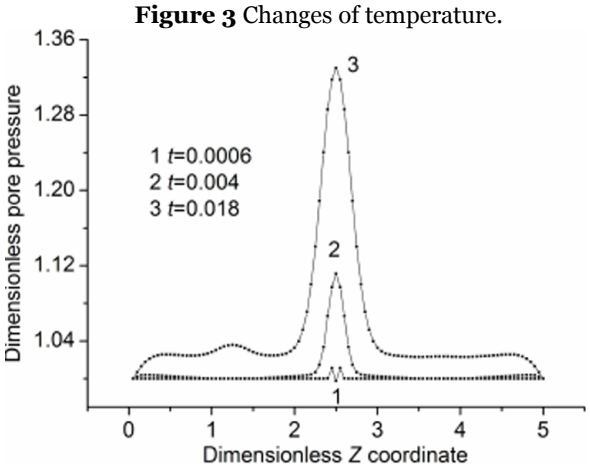

Figure 4 Changes of pore pressure.

most, which is called shear band. Inside shear band, pore pressure increases 160% and temperature increases about 23% in less than 0.1s during fast sliding. As a result, the friction and strength decrease fast and so landslide may easily happen.

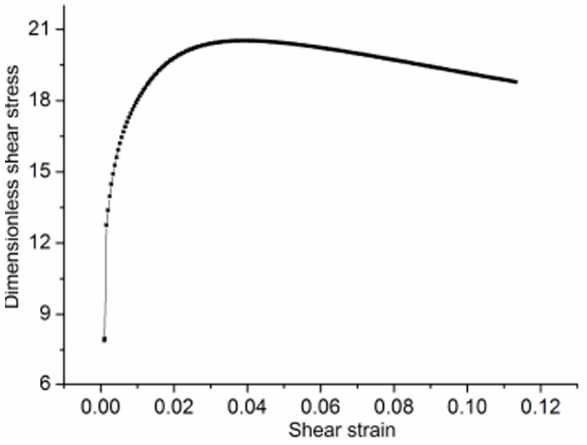

Figure 5 Development of strain and stress.

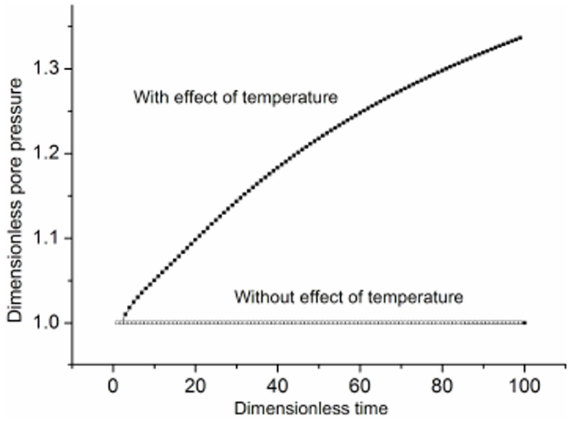

Figure 6 With and without effects of temperature.

Figure 5 shows the relationship of dimensionless shear stress and local shear strain at the center of shear band. It is shown that there is a peak in the curve of stress-strain. It is the typical characteristic of brittleness and dilatancy. In fact, only in dilatants slope, shear localization can occur. Shear band initiates just near the point that the stress began to decrease (Lu et al. 2012). The stress decrease can be explained by the pore pressure and temperature increase under shear load, so the softening effects overcome the effects of strain hardening at some time, just as Eq.(15) indicates.

Pore pressure increase under the effects of temperature can be several orders of magnitude more than that without temperature effects (Figure 6). The main reason is that on one hand heat can induce pore pressure increase directly, on the other hand heat can cause strain rate increase so as to produce more plastic work. Since the increase of pore pressure is one of the main reasons causing the decrease of soil strength, heat softening is an important factor to speed the failure of such clayey soil layer.

Plastic work ratio, $\tau\bar{\gamma}/2$, shrinks the shear band while the diffusion of pore pressure expands the shear band (Figures 7 and 8). It agrees with the theoretical results in literature (Lu et al. 2005) in tendency, but the development of shear band width is no longer in linear form.

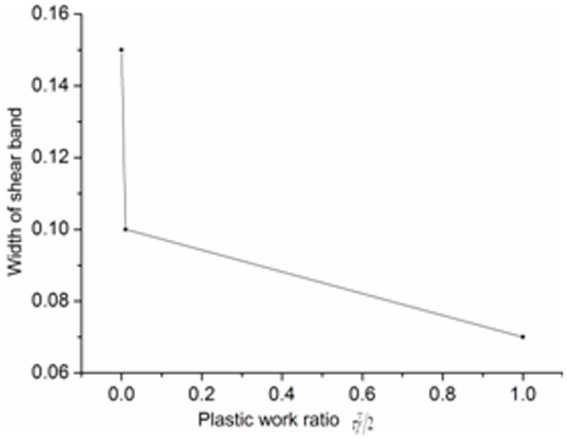

Figure 7 Effects of factor $\tau\bar{\gamma}/2$ on the width of shear band.

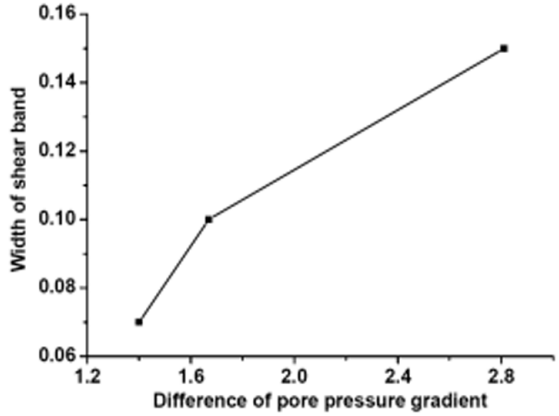

Figure 8 Effects of diffusion of pore pressure on the width of shear band.

The dynamic friction angle may decrease to φ_{dyn}=4.4° if the shear velocity increases (Tika and Hutchinson 1999). The friction coefficient can be expressed as the function of strain and strain rate.

$$\mu = \mu_r + (\mu_p - \mu_r)\frac{1}{1+a_1\dot{\gamma}} \quad (21)$$

$$\mu_r = \mu_p + (\mu_{sta} - \mu_{dyn})\frac{1}{1+a_2\gamma} \quad (22)$$

in which $\mu_{sta} = \tan\varphi_{sta}$, $\mu_{dyn} = \tan\varphi_{dyn}$, $\mu_p = \tan\varphi_p$, φ_{sta}, φ_{dyn}, φ_p are residual friction angles (respectively slow shear , fast shear, and the peak), and a_1, a_2 are constants.

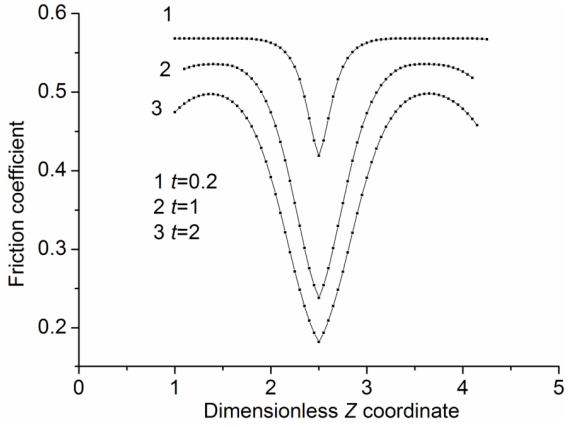

Figure 9 Changes of friction coefficient μ with time.

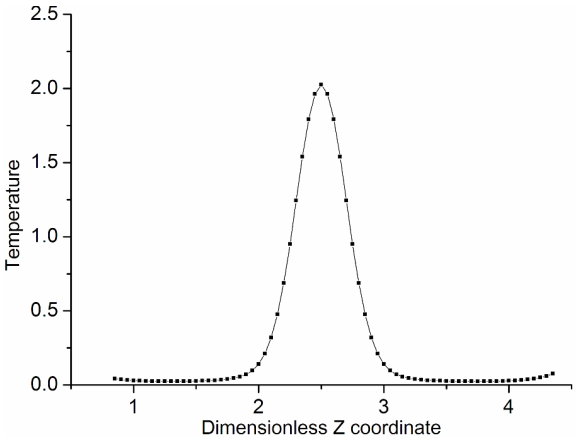

Figure 10 Temperature profile under shear.

Here, we adopt the data in literature (Vardoulakis 2002). φ_{sta}=10.15°, φ_{dyn}=4.4°, a_1=0.114, a_2=0.103. It can be seen from Figure 9 that friction coefficient gradually concentrates in the middle just as temperature and pore pressure with time. The reason is that strain and strain rate develop fast in the middle after the occurrence of shear band. So without the effects of pore pressure increase on the soil strength decrease, the friction coefficient decrease plays an important role in the weakening of soil.

To check whether the numerical analysis is consistent with experimental data, we have an analysis based on the data listed in the second paragraph of this section (Tika and Hutchinson 1999) and the shear velocity at the boundary is 0.1m/s and the specimen thickness is 0.02m. It can be seen from Figure 10 that the numerical rise in temperature inside shear band is about 2°C higher than that outside, that is, close to that given in literature by Tika and Hutchinson (1999).

3.3 Discussion

It can be seen from Eq.(19) that there are four dimensionless parameters controlling this problem: $f, \frac{C_v t_k}{\delta_k^2}, \frac{\lambda_m \theta_k}{p_k}, \frac{a\dot{\gamma}_0 t_k}{p_k}$, which denote plastic work-heat transition, thermal conduction, pore-pressure-heat transition and plastic work. Generally, thermal conduction is the slowest process relative to pore pressure dissipation and stress propagation. Stress propagation is the fastest in the three processes. So pore pressure increase due to heat can maintain while it will dissipate fast if plastic strain work is the only source of pore pressure increase. That is why the heat softening is so obvious. Plastic strain work can cause dilatancy and hardening and the increase of temperature and pore pressure. Temperature and pore pressure tends to decrease with dissipation. In some conditions, the heat softening will fully develop to overcome the strain hardening, which means that shear band will occur.

With thermal conduction towards outside the shear band, pore pressure increases and dissipates, the strength decreases with the increase of pore pressure, the softening zone thus tends to expand. Meanwhile, the shear strain induced dilatancy try to limit the failure zone in a small zone because of the volume increase and grains rearrangement. The occurrence of shear band and its expansion is both the interaction between heat and shear.

4 Conclusions

The thermal effects on the landslide with thin clayey layer are investigated. It is shown that the instability occurs once the thermal softening effects of soil overcome the strain hardening effects whether it is adiabatic or not. After instability, deformation is highly concentrated inside the shear band with a width of several centimeters at most, which causes the high strain

and strain-rate, the fast increase of pore pressure and heat inside the band, and fast decreases of friction. For example, temperature can increase more than 2°C, pore pressure can increase 160% in about 0.1s inside this zone. These changes cause the rapid decrease of friction coefficient to about 36% of the initial value in our simulation. These changes are deputy for the initiation of landslide in such kind of slopes.

The evolution of shear band width in a slope is determined by the dispersion of pore pressure and thermal, the soil strength. The former causes the band expansion while the latter the band shrinkage.

Acknowledgement

This study was funded by the National Natural Science Foundation of China (Grant No. 11272314; No. 51239010), the Specialized Research Fund for the Doctoral Program of Higher Education of China (Grant No. 20133514110004), and the Research Project of Chinese Ministry of Transport (Grant No. 201331849A130).

References

Goguel J (1978) Scale-Dependent Rockslide Mechanisms, with Emphasis on the Role of Pore Fluid Vaporization. Rockslides and Avalanches, In: Voight B (ed), Developments in Geotechnical Engineering 14A. Elsevier Scientific Publishing company, Amsterdam, Netherlands. pp: 693-705.

Hibib P (1975) Production of Gaseous pore pressure during rock slides. Rock Mechanics 7: 193-197.

Jean S, Stefanou I, Veveakis E (2011) Stability analysis of undrained adiabatic shearing of a rock layer with Cosserat microstructure. Granular Matter 13: 261-268. DOI: 10.1007/s10035-010-0244-1

Lu XB, Cui P, Hu KH (2010) Initiation and development of water film by seepage. Journal of Mountain Science 7(4): 361-366. DOI: 10.1007/s11629-010-2052-9

Lu XB (2001). The thermal-visco-plastic instability analysis of saturated soil. International Journal of Non-linear Mechanics, 36: 687-692. DOI: 10.1016/S0020-7462(00)00035-4

Lu XB, Jiao BT, Zhang JL et al. (2005) Thermo-effect on high speed landslide. Chinese Journal of Rock Mechanics and Engineering, 24(3): 424-429. (In Chinese)

Lu XB, Cui P, Chen XQ, Hu KH (2012) Evolution of shear zones using numerical analysis at the May 12th Wenchuan earthquake site, China. Environmental Earth Science 65: 1029-1036. DOI: 10.1007/s12665-011-1358-4

Lachenbruch AH (1980) Frictional Heating, Fluid Pressure and the Resistance to Fault Motion. Journal of Geophysical Research 85: 6097-6112. DOI: 10.1029/JB085iB11p06097

Moore R (1991) The chemical and mineralogical controls upon the residual strength of pure and natural clays. Geotechnique 41(1): 35-47.

Mass CW, Smith L (1985) Pore-Fluid Pressures and Frictional Heating on a Fault Surface. Pure & Applied Geophysics 122: 583-607.

Rice JR (2006) Heating and weakening of faults during earthquake slip. Journal of Geophysical Research 111: B05311 DOI: 10.1029/2005JB004006

Tika TE, Hutchinson JN (1999) Ring Shear Tests on Soil from the Vaiont Landslide Slip Surface. Geotechnique 49(1): 59-74.

Voight B, Faust C (1982) Frictional Heat and Strength Loss in Some Rapid Landslides. Geotechnique 32(1): 43-54.

Vardoulakis I(2000) Catastrophic Landslides due to Frictional Heating of the Failure Plane. Mechanics of Cohesive Frictional Materials, 5: 443-467. DOI: 10.1002/1099-1484(200008)5:6<443::AID-CFM104>3.0.CO;2-W

Vardoulakis I(2002) Dynamic thermo-Poro-Mechanical Analysis of Catastrophic landslides. Geotechnique. 52(3): 157-171. DOI: 10.1680/geot.52.3.157.41012

Veveakis E, Vardoulakis I, Toro G (2007) Thermoporomechanics of creeping landslides: The 1963 Vaiont slide, northern Italy. Journal of Geophysical Research 112: F03026. DOI: 10.1029/2006JF000702